FIP10604 – Text 16 – Magnetic measurements

Complementing our study of magnetism in solids, we present here, in a very superficial way, some of the main methods of magnetic measurements used in laboratory. This analysis is restricted to a few of the usual techniques, and limited to the description of their basic principles, without going into a detailed discussion of equipment.

Global methods

Methods belonging to this category essentially measure the total magnetic moment of a sample, using the result to determine magnetization and magnetic susceptibility (knowing the sample dimensions), also possibly to infer microscopic properties (knowing composition and crystal structure).

DC magnetometry

DC magnetic measurements are performed using a time-independent magnetic field. In general, series of measurements are made, either at fixed temperature for various applied fields, obtaining a curve $M(H)$, or keeping a weak (constant) applied field and varying the temperature to generate a curve $M(T)$. In this latter case, the ratio $M(T)/H$ should give the uniform susceptibility $\chi(T)$. Actually, one must take into account the demagnetizing field. As we discussed at the end of Text 15, defining $\chi_0 \equiv M/H$, the true susceptibility is given by $\chi = \chi_0/(1 - N_d\chi_0)$, where N_d is the appropriate demagnetization factor. In the PM phase, the obtained $\chi(T)$ values can be used, for instance, to fit a Curie-Weiss law at high temperatures.

The magnetic moment is determined by **force/torque** measurements, or by measuring magnetic **flux**.

- **Force measurements** are based on the fact that a magnetic moment $\boldsymbol{\mu}$, under the action of a **nonuniform** magnetic field associated to a magnetic induction $\mathbf{B}$, is subjected to a force $\mathbf{F} = (\boldsymbol{\mu} \cdot \nabla)\mathbf{B}$. Depending on the experimental setup, one can measure force or torque. The latter, being proportional to $\mathbf{M} \times \mathbf{B}$, allows access to the magnetization component perpendicular to the applied field, providing information on anisotropy axes.

- **Flux measurements** are performed by moving the sample along a straight line passing through or near pickup coils. The inductive effect of variation of magnetic flux through these coils affects the current carried by them in a precisely measurable way, allowing to determine the sample's magnetic moment. Usual setups are the *extraction magnetometer* and the *vibrating-sample magnetometer* (VSM). A scheme of the latter is shown in Fig. 1.

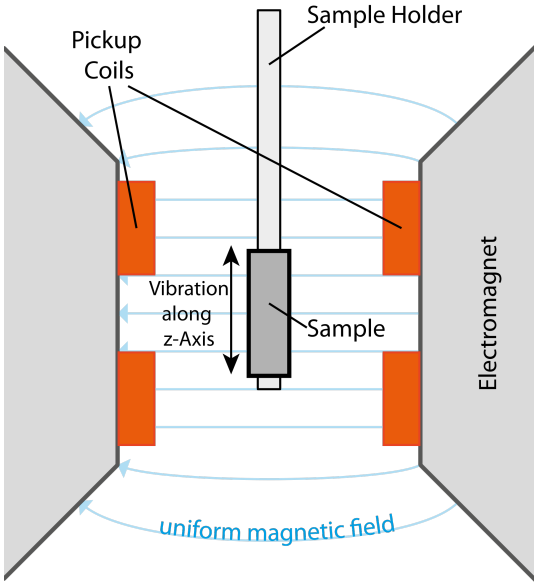

Figure 1 - Simplified scheme of a vibrating sample magnetometer (VSM).

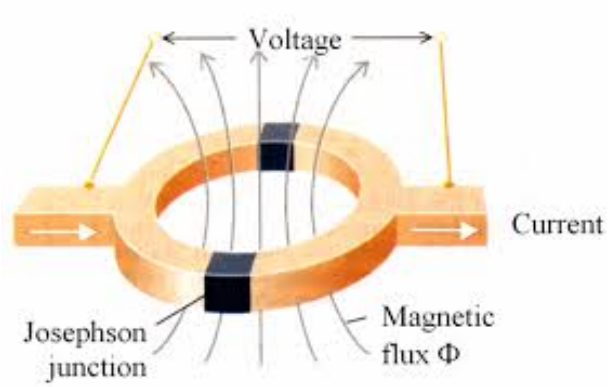

Figure 2 - Simplified scheme of the SQUID's operating principle, showing a superconducting ring with two Josephson junctions.

In a similar but more precise technique, the current induced by the sample motion is brought to a coil that generates a magnetic flux through a superconducting ring with Josephson junctions (see Fig. 2). Since the flux through a superconducting ring is quantized in integer multiples of the *magnetic-flux quantum* $\Phi_0 = he \simeq 2.07 \times 10^{-15}$ Wb, the current induced on the ring oscillates with a period Φ_0 as a function of flux. This is translated into an oscillating voltage under a bias current slightly larger than the small critical current of the junctions. The measuring device is known as SQUID (superconducting quantum-interference device).

AC magnetometry

Another kind of inductive method, instead of moving the sample, utilizes a small AC magnetic field superimposed to the uniform field that magnetizes the sample. This causes a time variation of the magnetic moment, with consequent magnetic-flux changes that are inductively detected by the pickup coils. The detection circuit filters the signal frequency, focusing on the frequency of the applied AC field.

Let us assume that the AC perturbing field has the form

$$h(t) = h_0 \sin(\omega_0 t)\,. \tag{1}$$

Its Fourier transform is

$$h(\omega) = i\frac{h_0}{2}\left[\delta(\omega-\omega_0) - \delta(\omega+\omega_0)\right]\,. \tag{2}$$

Assuming that the magnetization is parallel to the applied field, we can work with the magnitudes. Using the general relationship

$$M(\omega) = \chi(\omega)H(\omega) \tag{3}$$

it is easy to see that the alternating part of the magnetization is given by

$$M_{\rm AC}(t) = i\frac{h_0}{2}\left[\chi(\omega_0)e^{-i\omega_0 t} - \chi(-\omega_0)e^{i\omega_0 t}\right]\,. \tag{4}$$

Separating the real and imaginary parts of $\chi(\omega)$ in the form

$$\chi(\omega) = \chi'(\omega) + i\chi''(\omega)\,, \tag{5}$$

and taking into account that $M_{\rm AC}(t)$ is a real quantity, we verify that the real and imaginary parts of $\chi(\omega)$ satisfy the general relations

$$\chi'(-\omega) = \chi'(\omega)\,, \quad \chi''(-\omega) = -\chi''(\omega)\,. \tag{6}$$

From Eqs. (4) and (6) it follows that

$$M_{\rm AC}(t) = \left[\chi'(\omega_0)\sin(\omega_0 t) + \chi''(\omega_0)\cos(\omega_0 t)\right]\, h_0\,. \tag{7}$$

Thus we see that the "in-phase" and "out-of-phase" amplitudes of the signal give, respectively, the real and imaginary parts of the susceptibility at the applied-field frequency. Varying this frequency, one can determine $\chi(\omega)$ throughout a chosen frequency range.

The imaginary part of the susceptibility is associated to the power absorbed by the system. From the form of coupling between applied field and magnetic moments in the Hamiltonian, the power absorbed (per unit volume), i.e., the time-derivative of the magnetic energy, can

be written generically as $-\mathbf{M}(t)\cdot(\partial\mathbf{H}/\partial t)$. Using Eqs. (1) and (7), it follows that the time-averaged power is given by

$$\bar{P} = \tfrac{1}{2}\,\omega_0\,h_0^2\,\chi''(\omega_0)\;. \tag{8}$$

On the other hand, the fact that $\chi''(\omega)$ is odd with respect to a change of frequency sign implies that it vanishes when $\omega \to 0$. Therefore, in the low-frequency limit we have

$$M_{\rm AC}(t) = \chi\,h_0\sin(\omega t) = \chi\,h(t) \qquad \Rightarrow \qquad \Delta M(t) = \chi\,\Delta H(t)\;. \tag{9}$$

In this case, the sample magnetization follows a curve $M(H)$ and $\chi = dM/dH$ is the local slope of this curve, i.e., the (field-dependent) static susceptibility.

Observation of magnetic patterns

Some techniques are useful to visualize domain structures or study surface magnetization. We just mention the most common ones.

Magneto-optical techniques

- **Faraday effect -** It is observed in the **transmission** of plane-polarized light through a magnetic medium. If there is a component the magnetization along the direction of light propagation, there will be **rotation** of the polarization plane. It can be used in the case of transparent magnetic materials.
- **Kerr effect -** This again involves rotation of the polarization plane of light which in this case is **reflected** by a magnetized surface.

In both cases the effect is associated with spin-orbit interaction, which affects the transition probabilities between orbital states due to light that is **circularly** polarized clockwise or counterclockwise relative to the magnetization axis, thus changing their refractive indices. As a plane-polarized light can be decomposed into two circular polarizations of opposite senses, a change in refractive index causes rotation of the polarization plane.

MFM

This technique, called *Magnetic Force Microscopy* , consists basically in the use of *Scanning Probe Microscopy* (SPM) with a magnetic tip. Similar to what is done with an atomic force microscope (AFM), one records the intensity of the force exerted on the tip, which in this case is a magnetic force. Alternatively, one may work near a resonance frequency of the mechanical system to which the tip is attached (the vibration is activated, for example, by a piezoelectric crystal), and changes in the vibration frequency are recorded during the scanning. Since it is possible to apply a magnetic field during the measurement, changes of the domain structure under the applied field can be observed.

Local methods

Unlike the global methods discussed above, there are experimental techniques that allow to observe the spatial ordering of microscopic magnetic moments, even in the absence of an overall magnetization. We will discuss two of these techniques: neutron diffraction (the most employed) and Mössbauer effect.

Neutron diffraction

Diffraction methods are very useful in the analysis of periodic structures, as is well known, for instance, in the case of x-ray scattering to determine crystal structures. Simply stated, the key point is the interference condition

$$2\,d\,\sin\theta = n\lambda \qquad (n \text{ integer})\,, \tag{10}$$

which allows to measure the distance d between atomic planes contributing to constructive interference at a scattering angle 2θ for a given wavelength λ.

For magnetically ordered systems, since we want to determine the distribution of magnetic moments in space, we need a "radiation" that can interact magnetically, and has a wavelength comparable to typical interatomic distances. Neutrons are suitable for this purpose, as a neutron has an intrinsic magnetic moment and, in the case of thermal neutrons ($E \sim$ 5–100 meV), a wavelength in the range of 1–4 Å.

It is usual to make experiments with powder samples, for which all sets of properly oriented planes are found among the grains, contributing to the interference pattern at different angles. Instead of monochromatic beams, the *time-of-flight* technique can also be employed. It uses a **pulsed** source and fixed geometry, i.e., fixed angle θ and total (source-sample-detector) path L. Thus, the time of flight, measured from the beginning of the pulse to the moment of arrival at the detector, is directly related to the wavelength. As the pulse is polychromatic, different interference conditions (different d's for the same θ) are fulfilled at different times.

For non-magnetic systems or in the PM phase, neutron scattering is equivalent to x-ray scattering, except that neutrons are scattered by the atomic nuclei instead of the electrons. The scattering can be **elastic**, enabling determination of the crystal structure, or **inelastic**, when it gives information about the phonon spectrum.

When the system presents magnetic order, in addition to nuclear scattering there is a contribution from magnetic interaction with atomic spins. It is a magnetic dipolar interaction, whose general form was discussed in the beginning of Text 05. For a single-atom scattering event, the matrix element of the interaction potential between initial and final states of the neutron, which are essentially plane waves with wavevectors $\mathbf{k}$ and $\mathbf{k}'$, yields the scattering amplitude

$$V(\mathbf{q}) = \frac{4\pi}{q^2}(\boldsymbol{\mu}_\mathbf{q}\cdot\mathbf{q})(\boldsymbol{\mu}_n\cdot\mathbf{q}) - 4\pi\boldsymbol{\mu}_\mathbf{q}\cdot\boldsymbol{\mu}_n\,. \tag{11}$$

Here, $\mathbf{q} = \mathbf{k}' - \mathbf{k}$ is the wavevector transferred to the neutron, and $\boldsymbol{\mu}_\mathbf{q} = \sum_i \boldsymbol{\mu}_i \exp(i\mathbf{q}.\mathbf{r}_i)$, the sum being over the atomic electrons. The squared absolute value of $V(\mathbf{q})$ appears when one calculates the differential cross section in Born approximation. Averaging over all magnetic atoms (supposedly equal here), the final result can be written as

$$\frac{d^2\sigma}{d\Omega d\omega} = \text{const.} \sum_{\alpha\beta} (\delta_{\alpha\beta} - \hat{q}_\alpha \hat{q}_\beta) S_{\alpha\beta}(\mathbf{q}, \omega) \ , \tag{12}$$

where $\alpha, \beta = x, y, z$, $\hat{q}_\alpha$ represents a component of the unit vector $\hat{\mathbf{q}} = \mathbf{q}/|\mathbf{q}|$, and the quantity $S_{\alpha\beta}(\mathbf{q}, \omega)$ is the time Fourier transform of the correlation function

$$\mathcal{S}_{\alpha\beta}(\mathbf{q}, t) = \langle \mu^\alpha_\mathbf{q}(t) \mu^\beta_{-\mathbf{q}}(0) \rangle \ , \tag{13}$$

being therefore directly related to the dynamic susceptibility $\chi_{\alpha\beta}(\mathbf{q}, \omega)$. The frequency dependence is associated with the neutron's energy change upon scattering, $\Delta E_n = \hbar\omega$.

Focusing on elastic scattering, in the ordered phase $S_{\alpha\beta}(\mathbf{q}, 0)$ has a dominant contribution given by the square of the magnetization $M(\mathbf{Q})$, $\mathbf{Q}$ being the wave-vector that characterizes the magnetic order. The factor $(\delta_{\alpha\beta} - \hat{q}_\alpha \hat{q}_\beta)$ in Eq. (12) suppresses reflections for which the transferred wave-vector is parallel to the magnetization, allowing to infer its orientation in space. Subtracting the high temperature diffraction spectrum (only nuclear) from the low-temperature one gives the magnetic contribution, which reveals the kind of order that is established. On the other hand, the intensities of magnetic diffraction peaks allow to obtain the magnetization's magnitude. Then, experiments at different temperatures yield a curve $M(T)$.

Away from the Bragg condition (i.e., $\mathbf{q} \neq \mathbf{Q}$) there is no elastic scattering. However, inelastic-scattering peaks are observed for transferred energies corresponding to elementary magnetic excitations with those wave-vectors. Thus, we can obtain the magnon spectrum $\omega(\mathbf{q})$ by studying inelastic scattering for various wavevectors. When there is not a well defined resonance (e.g., when there is *damping* of excitations), the inelastic scattering gives information on the imaginary part of the dynamic susceptibility.

Mössbauer Effect

The Mössbauer effect is related to resonant emission or absorption of gamma rays in transitions between two nuclear states. A suitable isotope for the study of magnetic properties is ^{57}Fe, whose ground state and first excited state have nuclear spins 1/2 and 3/2, respectively. The importance for magnetism is on the Zeeman splitting of these states due to spin polarization of the atomic electrons, which allow to determine the intensity of magnetization at the ^{57}Fe site. A schematic representation of these levels, including the allowed transitions between them, is presented in Fig. 3.

There are two important effects to observe: *isomer shift*, which is the change in energy levels (different in the two states) caused by interaction of the electron cloud with the core

charge distribution; *quadrupole splitting*, which is the division of the nuclear-spin state $I = 3$ in two doublets ($I_z = \pm 1/2, \pm 3/2$) due to the nucleus quadrupole moment. The final splitting is caused by the effective magnetic field due to the spin polarization of the electrons of the atom, i.e., the local magnetic moment.

The observation of resonant absorption (which is the *Mössbauer effect*) is possible in solids because the recoil energy is very small, not exceeding the width of the excited state, which is about 10^{-8} eV (the energy difference between the two states in an isolated atom is 14.4 keV). Low temperatures are needed to avoid transitions accompanied by phonons. Furthermore, the small energy differences resulting from level shift or splitting have to be *compensated* by moving the source relative to the sample (Doppler shift). Typical relative speeds for ^{57}Fe are in the range of a few millimeters per second! When a resonance condition is reached, there is a sudden drop in the transmission, as seen in the bottom plot in Fig. 3. The six allowed transitions obey magnetic-dipole selection rules: $\Delta m_I = 0, \pm 1$. Only two minima would appear in the absence of magnetization.

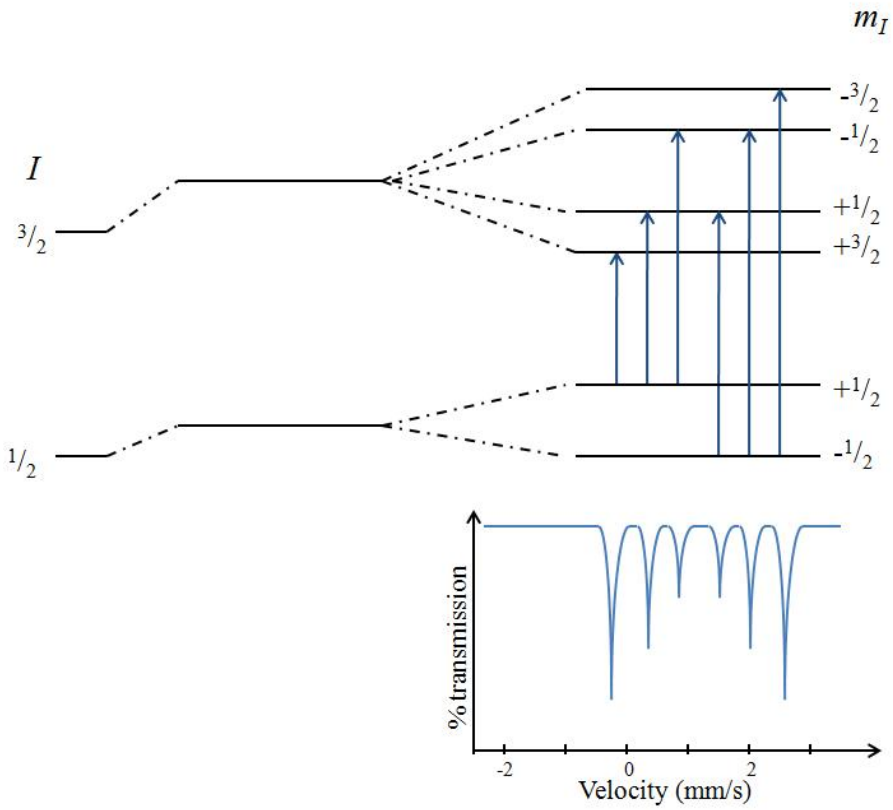

Figure 3 - Scheme of transitions between nuclear levels of ^{57}Fe with Zeeman splitting (top), and the corresponding gamma-ray absorption spectrum viewed as transmission intensity as a function of the relative velocity between source and sample (bottom).